ARTICLE

BIOTECHNOLOGY and BIOENGINEERING

A Simple Eccentric Stirred Tank Mini-Bioreactor: Mixing Characterization and Mammalian Cell Culture Experiments

David Bulnes-Abundis, Leydi M. Carrillo-Cocom, Diana Aráiz-Hernández, Alfonso García-Ulloa, Marisa Granados-Pastor, Pamela B. Sánchez-Arreola, Gayathree Murugappan, Mario M. Alvarez

Centro de Biotecnología-FEMSA, Tecnológico de Monterrey at Monterrey, Ave. Eugenio Garza Sada 2501 Sur, Monterrey, Nuevo León C.P. 64849, México; telephone: +52-8183-284131; fax: +52-8183-284136; e-mail: mario.alvarez@itesm.mx

ABSTRACT: In industrial practice, stirred tank bioreactors are the most common mammalian cell culture platform. However, research and screening protocols at the laboratory scale (i.e., 5–100 mL) rely primarily on Petri dishes, culture bottles, or Erlenmeyer flasks. There is a clear need for simple—easy to assemble, easy to use, easy to clean—cell culture mini-bioreactors for lab-scale and/or screening applications. Here, we study the mixing performance and culture adequacy of a 30 mL eccentric stirred tank mini-bioreactor. A detailed mixing characterization of the proposed bioreactor is presented. Laser induced fluorescence (LIF) experiments and computational fluid dynamics (CFD) computations are used to identify the operational conditions required for adequate mixing. Mammalian cell culture experiments were conducted with two different cell models. The specific growth rate and the maximum cell density of Chinese hamster ovary (CHO) cell cultures grown in the mini-bioreactor were comparable to those observed for 6-well culture plates, Erlenmeyer flasks, and 1 L fully instrumented bioreactors. Human hematopoietic stem cells were successfully expanded tenfold in suspension conditions using the eccentric mini-bioreactor system. Our results demonstrate good mixing performance and suggest the practicality and adequacy of the proposed mini-bioreactor.

Biotechnol. Bioeng. 2013;110: 1106–1118.

KEYWORDS: mini-bioreactor; eccentric; mixing; biotechnology; mammalian cell culture; stirred tank

Introduction

The biotechnology industry relies heavily on research at the laboratory scale and screening applications (Amanullah et al., 2010; Bareither and Pollard, 2011; Fernandes et al., 2011; Micheletti and Lye, 2006; Nienow, 2009; Wen et al., 2012). In order to determine the best formulation for a culture medium, the optimum temperature to run a culture process, or to identify the most productive clone from a pool of recombinant cells, a series of screening experiments is required. While stirred tanks are the most widespread bioreactor geometry in industrial biotechnology settings (Amanullah et al., 2004; Cascaval et al., 2004; Nienow, 2006, 2009), the first stages of any design or screening process are conducted in very small volume systems, in vessel geometries whose hydrodynamic behavior has nothing in common with that of industrial stirred tanks. Assay tubes, culture plates, Petri dishes, culture bottles, and Erlenmeyer flasks continue to be the preferred containers for the formulation of culture media, delineation and/or optimization of culture conditions, and growth and selection of high producer clones (Bareither and Pollard, 2011; Morga-Ramírez et al., 2010; Murugappan et al., 2010; Suresh et al., 2009; Wen et al., 2012). One problem is that the biological parameters determined or biological behaviors observed using these systems are not necessarily reproducible at the next scale—typically stirred tanks with a range of 0.5–1 L. Thus, there is an available niche for stirred tank-like cell culture systems for low to medium throughput screening, which could (at least partially) replace the traditional small-scale lab devices (from 5 to 100 mL) while assuring the reproducibility of relevant biological variables such as specific growth rate, cell densities, and viabilities (Ali et al., 2012; Zhang et al., 2010).

Cell growth is a complex process, where biological performance depends on multiple factors including oxygen mass transfer (Ali et al., 2012; Bareither and Pollard, 2011; Betts et al., 2006; Marques et al., 2010; Mou, 2010;

Correspondence to: M. M. Alvarez
Contract grant sponsor: Mexican government through CONACYT scholarships
Contract grant sponsor: Tecnológico de Monterrey at Monterrey through Cátedra de Investigación (CAT 122)
Received 3 August 2012; Revision received 19 October 2012; Accepted 25 October 2012
Accepted manuscript online 1 November 2012;
Article first published online 26 November 2012 in Wiley Online Library (http://onlinelibrary.wiley.com/doi/10.1002/bit.24780/abstract)
DOI 10.1002/bit.24780

Nikakhtari and Hill, 2006), temperature and pH control, nutrient availability, and so on. Most of these are highly influenced by mixing performance. Achieving good mixing in small volumes, however, is not a straightforward process (Ali et al., 2012; Bareither and Pollard, 2011; Wen et al., 2012). The typical stirred tank geometries used in industrial, pilot plant, or lab-scale biotechnology applications normally rely on turbulence as a mixing mechanism (Cascaval et al., 2004). Nonetheless, at smaller scales—that is in screening bioreactors—turbulence involves practical problems. While in 1 L tanks, agitation values in the range of 100–600 are sufficient to promote turbulent conditions in aqueous environments, in small systems, much higher agitation values are needed to achieve equivalently turbulent conditions.

To assure adequate oxygen mass transfer in a small-scale stirred tank is also difficult. In larger systems, agitation with turbines causes turbulence. Under turbulent conditions, oxygen dosed through fine spargers is correctly dispersed and typical bubble sizes and residence times allow for sufficient oxygen mass transfer. As the scale is reduced, a shorter residence time for air bubbles is expected, and adequate gas dispersion will demand higher shear rates. In addition, more bubbles per time unit will reach the surface of the tank, trapping cells at their surface. Both high shear rates and bubble bursting have been studied as possible factors for lethal and sub-lethal damage to mammalian cells (Amanullah et al., 2004; Chisti, 2000; Godoy-Silva et al., 2009; Keane et al., 2003; Nienow, 2006). This framework precludes the use of typical impeller designs and gas dispersion strategies for aerobic processes at very small scales. Hence, in stirred tanks, as the scale is reduced, gas transfer through the liquid surface becomes the ideal mechanism for gas–liquid mass transfer. However, in typical stirred tank geometries, the liquid surface/volume ratio is relatively low compared to that in Petri dishes, culture bottles, or Erlenmeyer flasks. Therefore, axial circulation and liquid surface renewal should be enhanced to make aerobic cell culture feasible in small-scale stirred tanks without using air bubbling (see also Mou, 2010).

In this study, we propose a simple stirred tank system to be used as a bioreactor for lab-scale and/or screening mammalian cell culture applications. Its mixing performance as a cell culture vessel is validated through experimental flow pattern visualization, computational fluid dynamics (CFD) simulations, and culture experiments using mammalian cells (CHO cells and hematopoietic stem cells).

Until recently, mixing in small-scale stirred tank bioreactors has scarcely been studied (Ali et al., 2012; Betts et al., 2006; Gill et al., 2008; Vallejos et al., 2005). The key differential geometrical aspect of this simple stirred tank is the off-centered (eccentric) position of its agitation shaft. In stirred tanks commonly used in industry and lab applications, the agitation axis is centrally located (concentric). However, the use of eccentrically agitated systems as mixing vessels has recently received research attention (Alvarez et al., 2002a; Ascanio et al., 2002; Cabaret et al., 2008; Galleti and Brunazzi, 2008; Hu et al., 2010; Karcz et al., 2005; Lai and Yang, 2010; Montante et al., 2006; Sánchez-Cervantes et al., 2006; Szoplik and Karcz, 2008; Takahashi et al., 2011; Yang et al., 2008, 2011; Woziwodzki and Jedrzejczak, 2010), although it has not been documented in the context of biotechnology applications.

Materials and Methods

Stirred Tank System

The stirred tank geometry studied here—a 30 mL effective volume glass round bottom vessel agitated using an angled-disc impeller—is depicted in Figure 1. The vessel was equipped with a heating jacket and its temperature is controlled by a water circulator (Model 1180S VWR®). Two aeration ports with 0.22 μm air filters were fitted in the tank lid. In this study, flow visualizations and mixing experiments were conducted by positioning the impeller (1 cm radius) at different eccentricities. Eccentricity (E) was defined as the ratio of the distance between the shaft and the vertical centerline of the tank (e) and the tank radius (R): $E = e/R$.

Flow Visualization Experiments

In all visualization experiments reported here, glycerin was used as a model fluid (viscosity equal to 1,100 cP at 25°C, measured with a Brookfield DV-E Viscometer). Mixing 3D patterns within the bioreactor were observed through fluorescent tracer injections (Fluorescein, FLUKA, PN: 46955) in a dark room where UV light (GE Blacklight F20T12/BL peaking at 370, 440, and 550 nm) was the only illumination source. To better describe the evolution of mixing in time, planar laser-induced fluorescence experiments (p-LIF) were conducted. In an otherwise dark room, a plane of laser light (Green 532 nm laser) was directed toward the experimental system to visually expose the mixing structure projected on a vertical 2D plane originated by the injection of a pulse of fluorescent dye, in this case rhodamine B (Sigma, Catalog number: 83689, absorption spectra peak around 550 nm). Time series were recorded at three frames per second (fps) using a professional digital camera (Canon® Rebel XTi). Images were processed using an image analysis software subroutine built in Python® to estimate the percentage of the total area covered by the dye at different times. Plots of the evolution of area coverage at different eccentricities and agitation values were constructed based on the analysis of each time series of images.

CFD Simulations

CFD was used to characterize flow behavior within concentric or eccentric stirred tank geometries. Simulations were done using an HP XW8600® Workstation with two Quad Core Xeon® processors and 16 GB of RAM. Geometries were

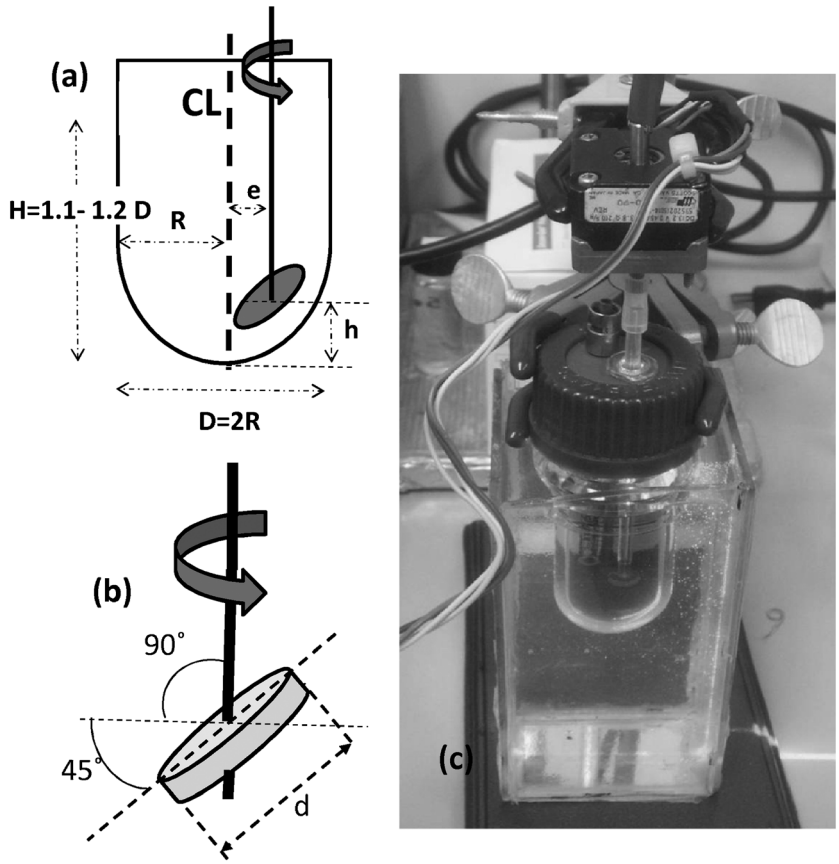

Figure 1. Schematic representation of the bioreactor system studied in this work: (**a**) a round-bottom tank agitated by an angled (45° angle with respect to the horizontal plane), eccentrically located (off-centered) disc impeller. The arrow indicates the direction of rotation of the axis; (**b**) details of the angled-disc impeller and; (**c**) view of the Actual system, including the motor drive and a squared chamber useful to correct for optical aberration (due to tank curvature) in p-LIF experiments.

built using SolidEdge® CAD/CAM Software, and meshes were constructed using software from ACUSIM® (acuMeshSim), which facilitated the generation of refined boundary layer elements on all model-critical areas. The resultant models consisted of 200,000–500,000 nodes and 1–3 million elements (depending on the specific case). The solutions of the velocity fields were calculated using ACUSOLVE from ACUSIM® Software Inc. (Mountview, CA). This code was based on a special stabilized Galerkin/least squares (GLS) finite element technology formulation of the full nonlinear Navier–Stokes equations. The liquid within the tank was modeled as a Newtonian fluid with the nominal properties of water. Based on the solution of the velocity field for each concentric or eccentric case, plots of velocity fields, shear stress distributions, and particle trajectories were constructed.

Cell Culture Experiments in the Eccentric 30 mL Bioreactor

Cell culture experiments were performed in a 30 mL eccentric reactor ($E = 0.42$) with a 45° angled-disc impeller for two different cell type models: A CHO–S cell line producer of a monoclonal antibody, and human hematopoietic stem cells (CD34+) isolated from the umbilical cord. For these experiments, agitation was provided by a 45° disc impeller (the same design used for the visualization experiment).

A series of CHO cell culture experiments (three replicates) was conducted using a chemically defined culture medium (CD OptiCHO°, from Gibco®, Invitrogen Cat Number. 12681–029). Dissolved oxygen and pH were not monitored or controlled. Agitation was set at 250 rpm. No air was bubbled into the tank, this allowed oxygen mass transfer to occur exclusively through the gas–liquid interface. The culture medium was changed on the fourth day, and the temperature was maintained at 37°C. Culture samples were taken every 24 h. To estimate cell viability, cells were stained with Trypan blue and counted using a Neubauer chamber. In these cultures, the specific growth rate during the exponential phase ($\mu = h^{-1}$) and the maximum cell concentration $[X]_{max}$ were calculated.

Human hematopoietic stem cells (CD34+) isolated from umbilical cord blood were cultured in DMEM F-12 (Invitrogen Cat. Number 12400–024 Carlsbad) supplemented with 10% FBS (Invitrogen Cat. Num. 16000–044, Carlsbad) and 1% penicillin–streptomycin solution (Sigma,

Cat. Num. P-4333, St. Louis) with 10 mM HEPES (Gibco, Invitrogen Cat Num. 11344-041, Carlsbad). pH and dissolved oxygen were not monitored or controlled. Agitation was set at 250 rpm. To allow oxygen mass transfer to occur exclusively through the gas–liquid interface, no air was bubbled into the tank. Cells were seeded at a concentration of 1.75×10^4 cells/mL. The culture medium (10% FBS, 1% penicillin–streptomycin solution, 10 mM HEPES) was changed every 24 h according to a fed batch protocol: agitation was suspended for 5 min to allow cells to settle in the bottom of the vessel, while 80% of the culture medium was removed from the upper portion of the tank using a sterile syringe and replaced by fresh medium at 37°C. One milliliter sample of cell suspension were removed for counting every 36 h. Cells were stained with Trypan blue at a concentration of 10% and counted using a Neubauer chamber.

Cell Culture Experiments Using Other Cell Culture Devices

Additional CHO cell culture experiments were carried out in (a) 6-well culture plates ($V = 2$ mL, with no pH or dissolved oxygen control); (b) Erlenmeyer flasks ($V = 125$ mL, with no pH or dissolved oxygen control); and (c) fully instrumented 1 L bioreactors (from DASGIP, Germany). In the bioreactors, agitation speed, temperature, and dissolved oxygen were set at 150 rpm, 37°C, and 30%, respectively.

Results and Discussion

Rationale of the Proposed Stirred Tank Geometry

Medium and large-scale bioreactors (from 1 to 10,000 L) rely on turbulence to homogenize. At small scales (namely 10–100 mL) turbulence is not necessarily the most efficient and cost-effective strategy to mix. For example, to achieve a similar degree of turbulence (equivalent *Re* value) within a 3 cm diameter reactor (such as the one studied here) and in a 10 cm diameter stirred tank operated at 80 rpm, we would need to agitate the small vessel at 866 rpm. This is neither feasible nor desirable. At this speed, the mechanical stability of the system would be questionable. Besides, when culturing shear-sensitive cells (i.e., mammalian, filamentous fungus, or plant cells) (Godoy-Silva et al., 2009; Keane et al., 2003; Kovnov et al., 2007; Morga-Ramírez et al., 2010; Nienow, 2006; Zhang et al., 2010) cell shear damage (lethal or sub-lethal) may occur.

The proposed stirred tank geometry (Fig. 1) relies on chaos instead of turbulence as the main mixing mechanism; furthermore, it is capable of producing good mixing even at very low rpm values (well into the laminar regime, $Re < 500$). Three geometrical features are crucial in the design of this mixing vessel: (a) the eccentricity of the impeller shaft, (b) the round bottom, and (c) the use of an angled-disc impeller. From these three elements, eccentricity is a determinant in defining a chaotic flow field (Alvarez, 2000; Alvarez et al., 2002a; Sánchez-Cervantes et al., 2006). Chaos is promoted by breaking time or space symmetries (Alvarez et al., 2002b; Alvarez-Hernández et al., 2002; Hobbs et al., 1997; Lamberto et al., 2001). A simple and effective way to disrupt flow symmetry in a stirred tank is by displacing the agitation shaft to an eccentric position (Alvarez et al., 2002a; Sánchez-Cervantes et al., 2006). However, in eccentric stirred tanks with flat bottom, segregated or low-rate mixing regions can be observed at the lower corners of the tank (Fig. 2a and b). In this study, the use of round-bottom geometries avoided lower corner segregated regions (Fig. 2c and d) and allowed for a smoother up-flow. Another modification introduced with respect to previous work employing eccentric stirred tanks was the use of a 45° angled-disk impeller. In the laminar regime, a simple horizontally oriented, concentrically located disk produces a fully regular flow with no convective mixing (Alvarez-Hernández et al., 2002; Arratia et al., 2005). As mentioned above, the same horizontal disc impeller (with no blades) produces chaos, and therefore mixing, when the axis of rotation is moved eccentrically (Alvarez, 2000; Alvarez et al., 2002a). However, the use of an angled impeller causes a more convoluted flow through at least two different means: (a) by exposing more surface area to displace fluid, acting practically as a bladed impeller; and (b) by adding a time-periodic perturbation to the already asymmetric system, creating a complex flow structure. Figure 2c and d illustrates the effects of an angled-disc impeller in the mixing structure.

Axial Flow Enhancement

Axial circulation in bioreactors is of great importance due to several key aspects: oxygen transfer, solid suspension, and dispersion of acid or base within the entire flow domain, among others. With respect to previous work (Alvarez et al., 2002a; Sánchez-Cervantes et al., 2006), these two geometrical modifications (round-bottom and angled-disc impeller) significantly improve mixing performance by increasing the impeller pumping capacity (axial circulation is significantly enhanced) and by eliminating segregation in the bottom region of the tank. Neither impeller inclination without eccentricity (Fig. 2e) nor the use of a round bottom and eccentricity with a horizontal disc impeller (Fig. 2f) is independently capable of producing equivalent mixing improvements.

Figure 3 shows the results from CFD simulations conducted using two different disc impellers: a flat horizontal disk similar to the impeller geometry previously analyzed by Alvarez et al. (2002a) and Sánchez-Cervantes et al. (2006) (Fig. 3; first column), and a 45° angled-disc (Fig. 3; second column). A Rushton impeller, the most commonly used radial impeller in mixing applications, is also included for comparison (Fig. 3; third column). In these simulations, stirring speed was set to 250 rpm in a fluid

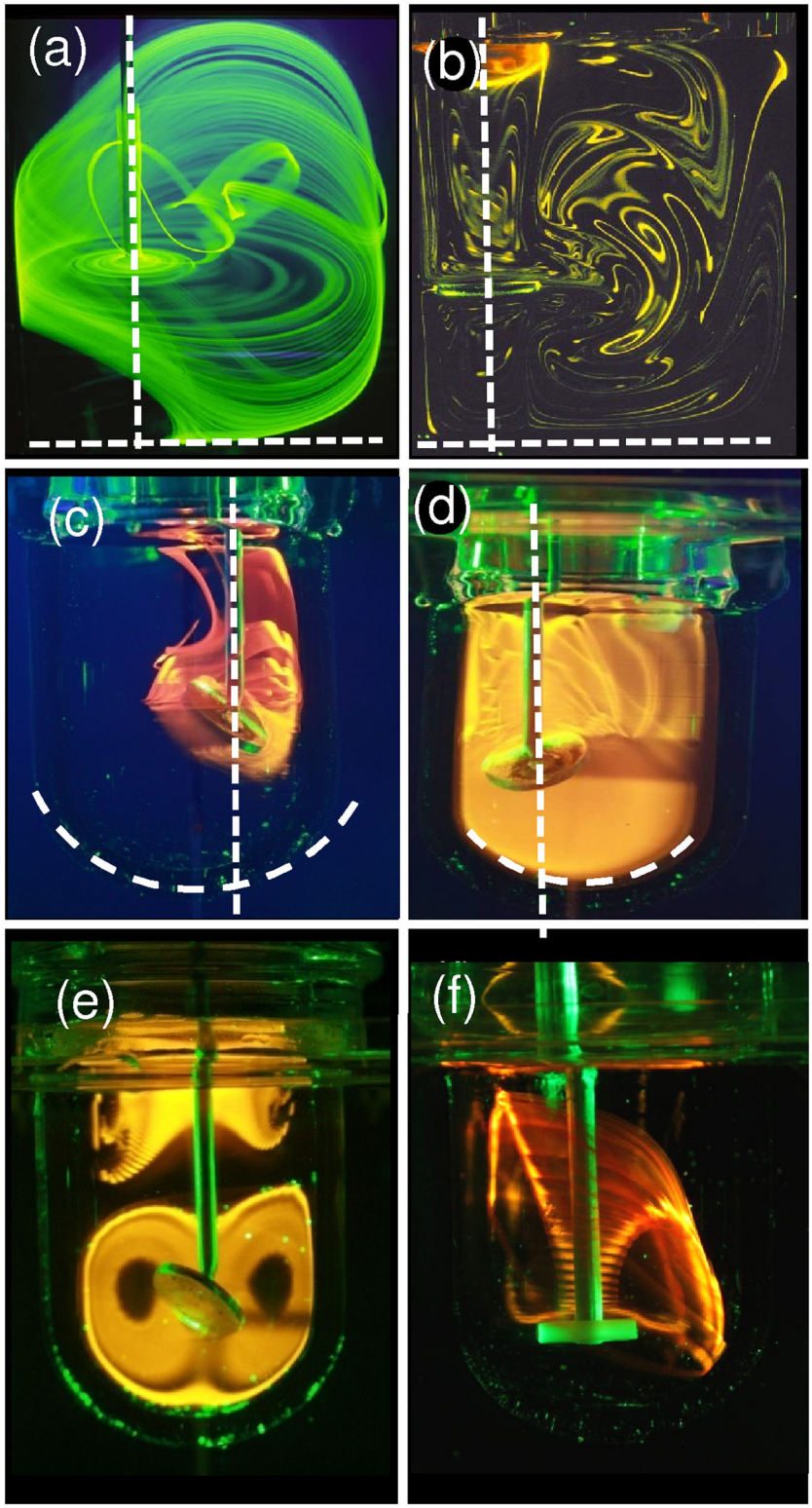

Figure 2. Mixing visualization experiments: (**a**) laminar flow patterns are revealed through a fluorescent tracer injection under UV light in an eccentric ($E=0.25$) and flat-bottom system 20 s after injection; (**b**) 50 s after injection (Alvarez et al., 2002a); (**c**) LIF experiments reveal the mixing structure of eccentric stirred tank systems agitated by a horizontal flat disc impeller; (**d**) a 45° angled-disc impeller at low Re ($Re \approx 0.37$); (**e**) a 45° angled-disc impeller concentrically located in a round-bottom tank ($Re \approx 0.37$); and (**f**) a horizontal flat disc impeller in a round-bottom tank.

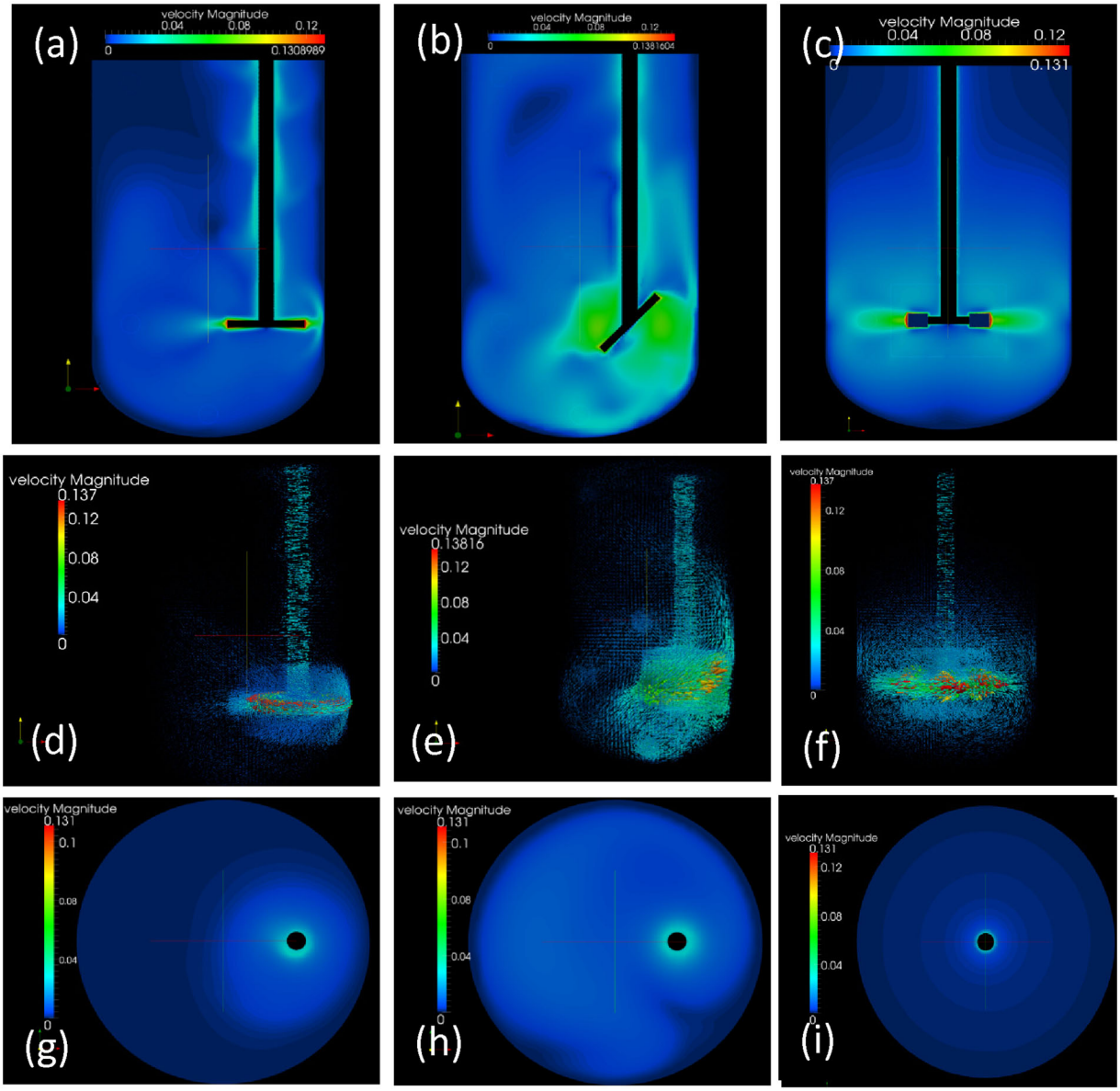

Figure 3. Velocity fields (as obtained by CFD calculations) in three different stirred tank configurations. Velocity magnitude contours within a vertical plane *XY* at $Z=0$ corresponding to a tank agitated by (**a**) a horizontal disc impeller located at $E=0.42$; (**b**) an angled-disc impeller located at $E=0.42$; and (**c**) a Rushton turbine located concentrically ($E=0.0$). Three-dimensional velocity vector plots indicate the area of influence of the impeller for the same three cases: (**d**) a horizontal disc impeller located at $E=0.42$; (**e**) an angled-disc impeller located at $E=0.42$; and (**f**) a Rushton turbine located concentrically ($E=0.0$). The velocity contours at a horizontal plane of the tank located slightly below the liquid surface (depth = 0.2 cm) show the effect of the impeller on the flow motion nearby the gas–liquid interface for (**g**) a horizontal disc impeller located at $E=0.42$; (**h**) an angled-disc impeller located at $E=0.42$; and (**i**) a Rushton turbine located concentrically ($E=0.0$).

matching the characteristics of water. Both disk impellers were located at an eccentric position ($E=0.42$), while the Rushton impeller was located concentrically. Circulation patterns and velocity fields significantly differ across systems. Velocity fields observed at the vertical tank mid-plane are compared in Figure 3a–c. The Rushton configuration induced a symmetrical flow with low velocity zones in the uppermost third of the tank (Fig. 3c; dark shade of blue). The flow field became asymmetrical when using eccentrically located disk impellers (Fig. 3a,b). Axial circulation was greatly improved by the use of an angled-disc impeller. In general, higher velocity values are observed in a vast region of the tank, and the low-flow velocity areas at the neighborhood of the liquid surface are substantially reduced (compare Fig. 3a–c). In mixing literature, it is customary to compare impeller/tank configurations in terms of pumping capacity (Q) and flow numbers (N_q). Through CFD, it is possible to calculate these quantities. For a 30 mL vessel, the pumping capacities for the horizontal and the angled disk impeller have been calculated at

1.4011×10^6 and $2.7831 \times 10^6\ m^2\ s^{-1}$, respectively (Bulnes-Abundis, 2012). Similarly, the flow number (N_q) for the horizontal and the angled-disc impeller were 0.336 and 0.639, respectively.

The 3D vector plots in Figure 3d–f further illustrate that the zone of influence of the impeller is considerably more extensive for the case of a tank agitated by the angled-disc eccentrically located. In particular, note the existence of an up-flow stream near the tank wall in Figure 3e. Comparatively, higher velocity magnitude vectors visit the bottom of the tank agitated by the angled-disc. This is of importance in the context of bioreactor engineering. Bioreactors are typically multiple-phase systems. The adequate suspension of cells in a stirred tank depends on the bottom circulation patterns. In addition, mass transfer through the liquid surface is governed by circulation patterns at the uppermost section of the tank. As mentioned previously (see Introduction Section), as the scale reduces, oxygen transfer through the liquid surface becomes the most feasible mechanism to deliver oxygen efficiently to aerobic cultures. Figure 3g–i presents velocity fields corresponding to a horizontal plane located 0.2 cm below the liquid surface. Higher velocity values near the surface are observed when the 45° angled-disc impeller is used (Fig. 3h).

Destruction of Flow Separation Planes

In the laminar regime, concentric tanks agitated with typical axial (Alvarez et al., 2002a), or radial impellers (Alvarez et al., 2005; Cabaret et al., 2008) exhibit extremely impermeable flow separation planes at the impeller height that practically convert the top and bottom sections in independent reactors from the convective point of view (Alvarez et al., 2005; Sánchez-Cervantes et al., 2006; Zalc et al., 2002). At eccentricity values higher than 0.30, the top–bottom separation is destroyed and therefore, top–bottom circulation is greatly facilitated. Here, we present results from CFD simulations where 125 mass-less particles were located at an initial condition above (Fig. 4a) or below (Fig. 4b) the impeller plane of a tank agitated by a concentrically located Rushton impeller. In the range of Reynolds numbers (Re) from 0.1 to 416, particle streamlines remain confined to the tank section where particles are seeded. In addition, as a consequence of the flow field, solid particles (e.g., cells) tend to be driven to the deepest point of the tank. The ascending local velocities that prevail at these locations are low (as seen in Fig. 4b). Therefore, some solid particle deposition is expected in this zone.

In contrast, in an eccentrically agitated system (Fig. 4c), particle trajectories explore practically the entire flow domain. The flow structure at the bottom of an eccentric system sweeps the tank surface with circulatory trajectories and, for the same rpm value, achieves higher local velocities (Fig. 4c). In addition, the center of the circulatory pattern at the tank bottom is not located at the deepest point of the tank. The circulatory motion at the bottom minimizes the problem of particle settlement and potentially reduces the just suspension velocity required for a particular particle size and density. In our experiments with cellular suspensions, the just suspension velocities of mammalian cell suspensions (CHO and hematopoietic cells) were always found to be lower in eccentric systems than their concentric counterparts.

The results presented in Figure 4 provide additional evidence of the improvement of axial circulation near the gas–liquid interface in eccentric systems. For the same rpm

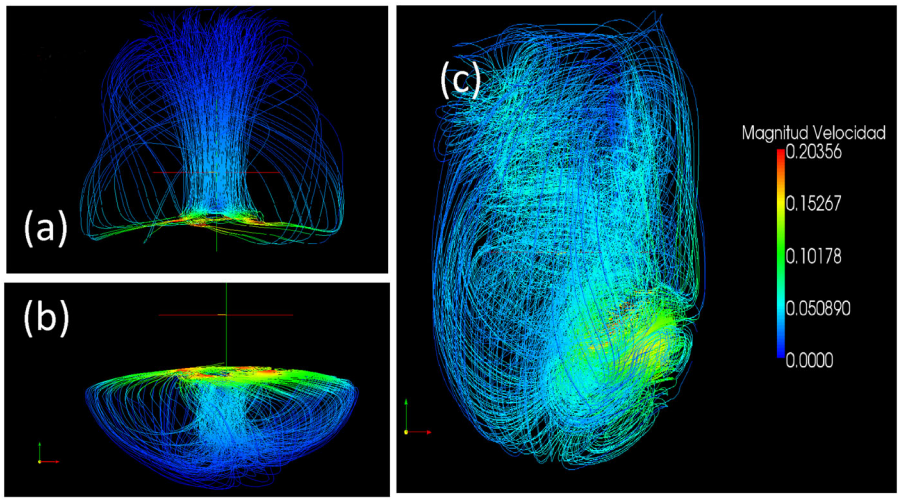

Figure 4. Particle trajectories in concentrically and eccentrically agitated stirred tanks calculated using CFD. In each case, 125 mass-less particles were located in an initial condition, and their trajectories were followed for 7.6 s of impeller revolutions. Three cases are presented: (**a**) a tracer initially located above the impeller plane of a tank agitated at 250 rpm by a conventional Rushton impeller located concentrically; (**b**) a tracer initially located bellow the impeller plane of a tank agitated at 250 rpm by a conventional Rushton impeller located concentrically; and (**c**) a tracer initially located above the impeller plane of a tank agitated by a 45° angled-disc impeller located eccentrically ($E = 0.42$) at 250 rpm.

values, the frequency of trajectory visitation to the fluid surface is higher in eccentric systems (compare Fig. 4b,c). In addition, in concentric systems, the fluid–gas interface is more frequently visited in the central region of the tank, in the vicinity of the impeller shaft. A much lower visitation frequency is observed in the neighborhood of the tank walls. In the eccentric case, the visitation area at the gas–liquid interface is not restricted to the central region (in Fig. 4c). This improvement in axial circulation suggests a positive effect in terms of mass transfer enhancement from the head space (this has not been formally quantified here).

Shorter Mixing Times

Different eccentricity values and agitation speeds have a different effect on mixing structure and mixing time (Alvarez, 2000). Figure 5a–d presents the evolution of the mixing structure in a stirred tank containing glycerin with an eccentricity value $E = 0.42$ operated at 200 rpm. We used pure glycerin (viscosity $\approx$ 1,100 cP) as a model fluid to minimize the effects of diffusion (its use allows experimental "decoupling" of convective and diffusive mixing), and to slow down convection for better observation of structural features and mixing behavior over a time span of minutes rather than seconds. Below, we will extrapolate our observations to the context of aqueous environments typical of bioreactors. Under our experimental conditions, the flow was laminar ($Re < 1.0$) and the mixing structure developed quickly. Five minutes after the dye injection, essentially 95% of the observed tank plane had been covered by dye. From this observation, the mixing $\text{times}_{95\%}$ can be estimated as approximately 5 min for $E = 0.42$ at $Re < 1$. Figure 5e–g presents the evolution of the mixing structure, calculated from LIF experiments, for other eccentricity values. At $E = 0.0$ (the concentric case), complete mixing

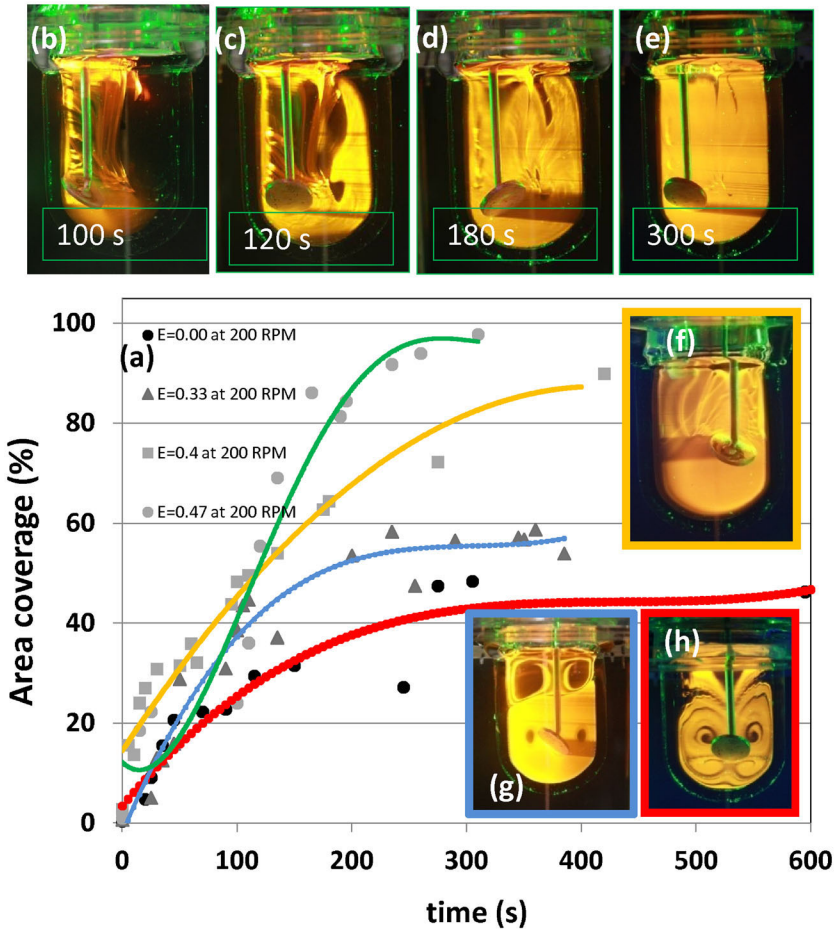

Figure 5. Mixing proceeds at different rates and reaching different extents (in terms of the total volume of the system) at different eccentricity values. (**a**) The evolution of the mixing (measured by p-LIF experiments as area coverage at different times) is presented for a tank agitated at 200 rpm by a 45° angled-disc located at different eccentricity values: concentrically (●); $E = 0.33$ (▲); $E = 0.40$ (■); and $E = 0.47$ (●). Visualization of the evolution of mixing in a round-bottom stirred tank agitated by a 45° angled-disc eccentrically located ($E = 0.47$) at the following different times after a fluorescent tracer injection: (**b**) 90 s, (**c**) 120 s, (**d**) 180 s, and (**e**) 300 s. In concentric and low-eccentricity cases, incomplete mixing is observed even after long agitation times: (**f**) in the concentric case ($E = 0.0$) incomplete mixing was observed after 600 s; (**g**) at $E = 0.33$, incomplete mixing is observed after 400 s; and (**h**) at $E = 0.40$, approximately 90% of the cross-sectional area of the tank was invaded by the tracer injection after 400 s.

was not achieved in the period of observation. After 10 min of agitation, less than 50% of the illuminated plane had been covered with fluorescent dye; therefore, a mixing $times_{95\%}$ could not be estimated. A remarkably symmetric structure is observed. The toroidal regular regions characteristic of laminar concentric stirred tanks (Lamberto et al., 1999, 2001) and a separation plane at the impeller level are evident. Similarly, previous LIF studies in laminar tanks concentrically agitated by radial Rushton turbines (Alvarez et al., 2002b) and axial four-bladed impellers (Alvarez et al., 2002a) reported the existence of toroidal segregation and separation planes. At eccentricity $E = 0.33$, mixing is significantly improved, yet segregation survives after six minutes of agitation, particularly in the top section of the tank. In general, we observed that eccentricity values in the range of $E = 0.40$–0.47 render flows with practically no segregated areas (globally chaotic flows) with mixing $times_{95\%}$ in the order of 6–8 min at $Re < 1$. Similarly, in experiments performed in the laminar regime ($Re = 1.5$–13.0; using a radial impeller), Cabaret et al. (2008) reported the occurrence of practically complete mixing (as evaluated by a similar technique) only in the narrow window of eccentricity values from $E > 0.257$ to $E > 0.56$ and $7.5 < Re < 13.0$. Indeed, for the lowest Re value where complete mixing was observed ($Re = 7.5$), E values in the range of $E = 0.39$–0.56 were required. Sánchez-Cervantes et al. (2006) also studied the mixing performance of a flat-bottom eccentrically agitated laminar stirred tank using glycerin as a model fluid. The authors estimated relatively short mixing times (in the order of 5–6 min) for a stirred tank with a 1,000 mL volume agitated with a 3 cm diameter horizontally oriented disc at 500 rpm ($Re \approx 15$).

The studies of Sánchez-Cervantes et al. (2006) (with horizontal-disc impellers) and Cabaret et al. (2008) (with radial impellers) were performed in larger systems (see Table I). Only a few authors have studied mixing in mini-bioreactors (e.g., Vallejos et al., 2005). In Table I, we list and compare the experiments from Sánchez-Cervantes et al. (2006), Cabaret et al. (2008), and Vallejos et al. (2005) were mixing times were estimated for laminar mixing systems, versus those conducted in this study. The use of eccentricity, a round bottom, and an angled-disc impeller result in practically complete mixing at the lowest Re values (in comparison with other impeller and tank configurations). Lower dimensionless mixing times are achievable using other configurations (eccentric radial impellers as in Cabaret et al. (2008) or a concentric radial impeller as in Vallejos et al. (2005)), but at much higher Re values. In the context of mixing in mini-bioreactors, this suggests that the stirring configuration studied here would provide adequate mixing in smaller vessels at lower rpm values (and lower tip speed values; see Table I) than other systems. This can be very useful in the context of the small-scale culture of shear-sensitive cells such as CHO cells, stem cells, plant cells, and fungus broths, since a common consideration in the scaling of shear sensitive cells is not to exceed the maximum tip speed (πND). Based on the data presented here, the assumption of a linear relationship between dimensionless mixing time and Re (in the laminar regime), and considering the typical kinematic viscosities of culture media (approximately 1.0 unit), similar mixing times (in the order of minutes) will be expected in the small-scale bioreactor at less than 1 rpm. Alternatively, with agitations of 200–300 rpm, mixing times in the order of seconds are anticipated using eccentric mini-reactors. In practice, this means adequate mixing at lower power input and shear stress. For example, in our 30 mL eccentric bioreactor systems (at $E = 0.42$; $N = 250$ rpm; $Re > 1$), mixing times are achieved in 5 min and the maximum tip speed values are 18× lower than those anticipated if a horizontal-disc is used (see Table I).

Power Consumption and Shear Stress Distributions

So far, we have presented evidence of adequate mixing performance at low Re numbers. Intuitively, this implies lower shear stress for the same mixing efficiency (since mixing is achieved at lower rpm values). Remarkably, we found that the eccentric/angled-disc configuration studied here induces lower shear stress than a conventional

Table I. Mixing time experiments in different laminar stirred tanks configurations.

Exp.	D_{tank} (cm)	N (RPM)	Re	E	d_{disc} (cm)	πND (cm/min)	M_{time} (min)	Reference	Re_i/Re_j	ND_i/ND_j	$(N)(t_{mixing})$
1	9.00	150	4.5	0.42	3	1,413.72	60	Sánchez-Cervantes et al. (2006)	6.75	2.25	9,000
2	9.00	300	9	0.42	3	2,827.44	20	Sánchez-Cervantes et al. (2006)	13.50	4.5	6,000
3	9.00	500	15	0.42	3	4,712.40	6	Sánchez-Cervantes et al. (2006)	22.50	7.5	3,000
4[a]	3.00	200	0.7	0.47	1	6,28.32	6	This study	1.00	1	1,200
5	3.00	150	0.5	0.47	1	471.24	7	This study	0.75	0.75	1,050
6	3.00	200	0.67	0.4	1	628.32	15	This study	1.00	1	3,000
7	21.50	516	7.5	0.41	6.53	10,585.56	4.85	Cabaret et al. (2008)	11.25	16.8474	2,502.6
8	21.50	516	7.5	0.51	6.53	10,585.56	1.94	Cabaret et al. (2008)	11.25	16.8474	1,001.04
9	21.50	516	7.5	0.56	6.53	10,585.56	1	Cabaret et al. (2008)	11.25	16.8474	516
10	1.70	34	25	0	0.9	95.69	3.583	Vallejos et al. (2005)	37.50	0.15	121.28

Data collected in this study (rows 4, 5, 6) is compared to the results from experiments reported in literature. Experiments were conducted in different model fluids but are comparable in terms of dimensionless quantities. Experiments 1–6 were conducted in glycerin, 7–9 in a concentrated corn syrup solution, and experiment 10 in water.

[a]Case taken as reference for the calculation of fold-increase in Re_i/Re_j and ND_i/ND_j.

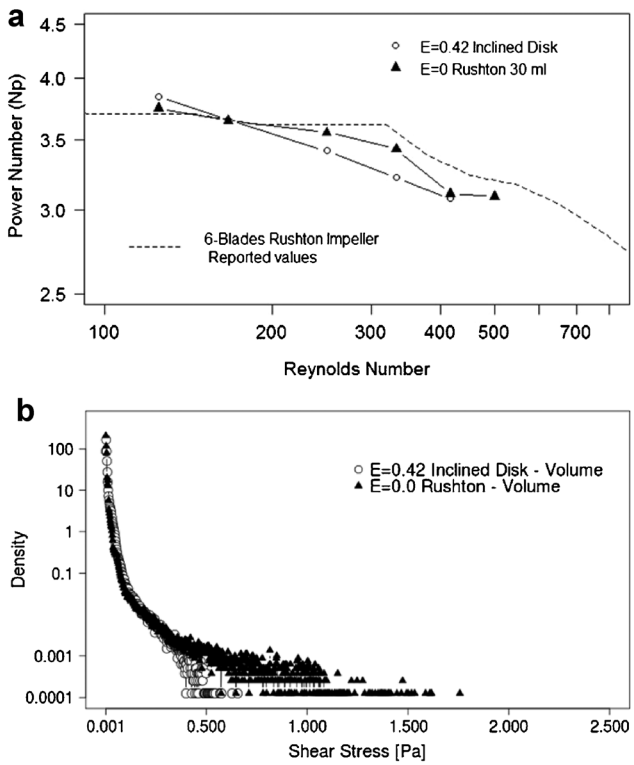

Figure 6. (**a**) The relationship between the power number (*P*) and Reynolds number (*Re*), as calculated by CFD, for the case of a tank agitated by a Rushton turbine located concentrically (-▲-); and a tank stirred by an angled-disc eccentrically located at $E = 0.42$ (-○-). For comparison, data from the literature is presented for the Rushton/concentric configuration (—). (**b**) Shear stress distributions, calculated in a grid of 100,000 points distributed in the plane *XY* at $Z = 0$ for a Rushton turbine located concentrically (-▲-), and a tank stirred by an angled-disc eccentrically located at $E = 0.42$ (-○-).

concentric/Rushton configuration, even at the same *Re* values (and equivalent power numbers). Figure 6a shows power number values as a function of *Re*, estimated using CFD, for a tank agitated by an eccentrically located angled-disc and a concentric Rushton. The data suggest that both systems are practically equivalent in terms of power consumption for the same *Re*. Figure 6b shows shear stress distribution at $Re = 416$, calculated from CFD simulations, for an eccentrically located angled-disc and a concentric Rushton. Even at the same *Re* value, the shear stress distribution inherent to the eccentric/angled-disc system is narrower and contains a significantly lower frequency of high shear stress values.

In the following section, we present results from actual mammalian culture experiments that demonstrate the use of eccentric mini-reactors in relevant biotechnological settings.

CHO Cell Culture Experiments

Chinese hamster ovary (CHO) cells are the most commonly used mammalian host for the commercial production of therapeutic glycosylated proteins (Kim et al., 2012; González-Leal et al., 2011). In this section, we present data derived from batch CHO cell culture experiments conducted in a 30 mL eccentrically agitated mini-bioreactor (30 mL-EB). In addition, we compare this data versus that obtained in other relevant bioreactor types: 6-well microplates (6-W), Erlenmeyer flasks (30 mL-EMF), and fully instrumented 1 L stirred tank bioreactors (FIB). Six-well microplates and Erlenmeyer flasks are among the most commonly used platforms for CHO cell culture work at the lab scale. On the other hand, a 1 L stirred tank instrumented bioreactor would be one logical "next stage" in the process of design and scaling-up of a CHO cell culture process. A reliable lab-scale bioreactor will ideally produce similar data than other systems at the same scale. And most importantly, it should predict relevant indicators to be observed at other scales with lower effort (lower cost and lower instrumentation demands, etc.). Figure 7a shows the cell count profiles for experiments where 2.5×10^5 CHO cells were seeded in the 30 mL-EB operated at 250 rpm with no pH control. No

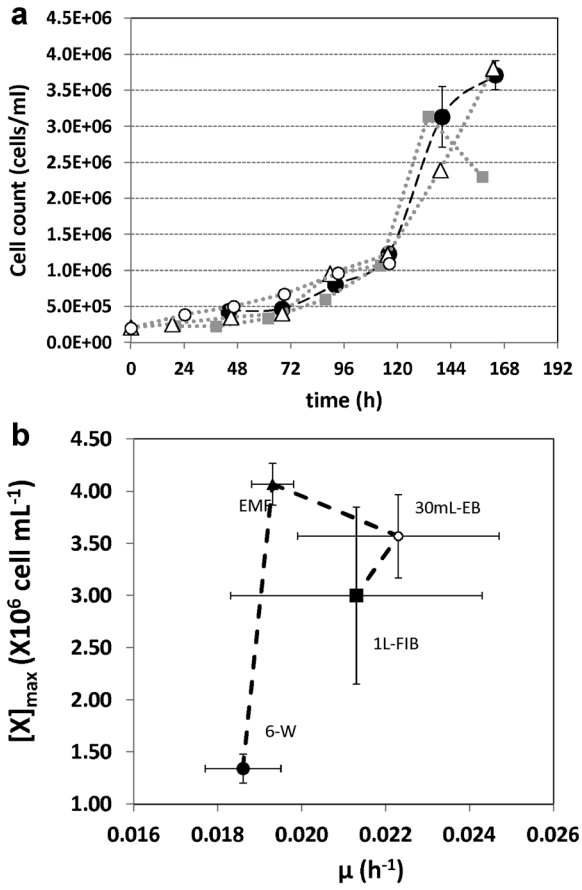

Figure 7. Culture of CHO cells in 30 mL eccentrically agitated bioreactors. Different aspects of the culture of CHO cells are shown: (**a**) cell growth of CHO cells in a batch culture; (**b**) bi-dimensional plot of the specific growth rate (μ) and maximum cell density $[X]_{max}$ of the culture in four different culture systems—6-well culture plates (6-W), Erlenmeyer flasks (EMF), eccentrically agitated 30 mL bio-reactors (30 mL-EB), and 1 L fully instrumented bioreactors (1L-FIB). Three experiment replicas are plotted. Error bars indicate standard deviation of each data point.

air was bubbled into the tank, which allowed oxygen mass transfer to occur exclusively through the gas–liquid interface. The exponential growth phases of the three growth cultures were overlapped. Although the extent of the lag phases varied between these experiments (not shown), remarkable consistency was observed during exponential growth (Fig. 7a). In addition, a similar evolution of cell densities over time was observed in eccentrically agitated mini-bioreactors and fully instrumented bioreactors. Growth curves derived from experiments conducted in 1L-FIB (using the same cell strain and culture media) are also presented in Figure 7a. Although with higher dispersion, these growth curves closely follow the evolution observed in 30 mL-EB. Specific growth rates calculated from experiments in the four different culture systems are presented in Table II and graphically compared along the x-axis of Figure 7b. The μ values derived from the 1L-FIB exhibited the highest standard deviation (denoted by the error bars), statistically covering any significant difference with respect to estimates from lab-scale systems. However, among small-scale systems, μ values derived from 30 mL-EB are statistically higher than those observed in EMF and 6-W, and closer to the average μ value observed in 1L-FIB. Another relevant biological indicator, the maximum cell density $[X]_{max}$ was also compared among culture systems. In Table II and Figure 7b (y-axis), the $[X]_{max}$ observed in different culture systems are compared: 1L-FIB and 30 mL-EB were statistically equivalent in terms of $[X]_{max}$, although a highest standard deviation (see error bars) was observed for the case of experiments in 1L-FIB. However, in 6-W plates, statistically lower $[X]_{max}$ values were observed (they also showed the lowest growth rates; Fig. 7b). In EMFs ($V_{effective} = 125$ mL), the statistically highest $[X]_{max}$ values were measured. In summary, considering both parameters (μ and $[X]_{max}$), 30 mL-EBs were the small scale system that performed the most similarly to 1L-FIBs (see Fig. 7b). The $[X]_{max}$ measures in 30 mL-EB and 1L-FIB were both similar to those observed in full commercial-scale operations (in the order of 5×10^6 cells/mL; Nienow, 2006). We also ran CHO cell culture experiments in 30 mL concentric bioreactors. Consistency among these experiments was poor. Although we observed similar specific growth rates in both concentric and eccentric tanks, the concentric configurations gave a lower $[X]_{max}$, no higher than 1.90×10^6 cells/ml. (The average $[X]_{max}$ in the eccentric bioreactors was 3.7×10^6 cells/mL). We attributed this lack of reproducibility and diminished performance to mixing issues. For instance, in eccentric tanks, cells were completely suspended at 200 rpm. In contrast, in concentrically agitated systems, also agitated at 200 rpm, a significant fraction of the cells remained settled on the tank bottom.

The selection of 250 rpm as the agitation value for our experiments in the 30 mL-EB deserves some discussion. The geometrical features (of the tank and the impeller), and inclusively the main mechanism for oxygen transfer, were different in the 30 mL-EB and the 1L-FIB. Therefore, scaling-down by matching power per unit of volume (P/V) would not have physical grounds. On the other hand, CHO cells have been described as shear sensitive (Chisti, 2000; Godoy-Silva et al., 2009; Keane et al., 2003). Therefore, constant maximum tip speed (πND) among scales could be a reasonable criterion to dynamically compare both systems. Please note that the criterion of similar maximum tip speed is adequate for small-scale systems. However, scaling up at constant tip speed above the 1L-scale will not be advisable since the power/volume will drop drastically and, consequently, so will the mass transfer coefficient. A scale-down calculation considering the impeller diameter and agitation rate used at 1L-FIBs (and accepting that both tanks are not geometrically similar) will result in an agitation rate of 550 rpm in the 30 mL-EB. Our results suggest that the agitation value of 250 was enough to properly attend the mass transfer demands of the culture during exponential phase.

Stem Cell Culture Experiments

Massive stem cell expansion has been recognized as a bottleneck for the development of feasible tissue engineering treatments. The culture of stem cells in stirred tank bioreactors has only recently been explored (Kowalczyk et al., 2011; Rodrigues et al., 2011; Want et al., 2012). In our experiments with hematopoietic stem cells, agitation was set at 200 rpm to allow for adequate mixing while minimizing damage induced by mechanical stress. Although adequate liquid–liquid mixing is achievable at much lower speeds, visualization experiments with neutrally buoyant 250 micron particles (results not presented here) demonstrate that higher speeds are needed to hold cells in suspension. The just suspension velocity for polystyrene particles in water was estimated in 200 rpm. Cells cultured in the eccentric stirred tank bioreactor at an initial concentration of 1.75×10^4 cells/mL exhibited growth curves (Fig. 8) with characteristic latency, exponential, and stationary phases. Cell doubling time, calculated using a linear regression analysis

Table II. Specific growth rates (μ) and maximum cell concentrations $[X]_{max}$ of CHO cell cultures observed in different screening systems.

Reactor type	Scale (mL)	μ (h^{-1})	Max cell density (cell/mL)	Observations
6-well culture plates (6-W)	8	0.0186 ± 0.0009	$1.34 \pm 0.14 \times 10^6$	Seven day culture; no pH or DO control; $T = 37°C$
Erlenmeyer flask (EMF)	30	0.0193 ± 0.0005	$4.07 \pm 0.20 \times 10^6$	Seven day culture; no pH or DO control; $T = 37°C$
Eccentric 30 mL bioreactor (30 mL-EB)	30	0.0223 ± 0.0024	$3.57 \pm 0.25 \times 10^6$	Seven day culture; no pH or DO control; $T = 37°C$
DASGIP reactor (1L-FIB)	1,000	0.0213 ± 0.0030	$3.01 \pm 0.848 \times 10^6$	Fully instrumented bioreactor; pH 7.0; DO = 20%; $T = 37°C$

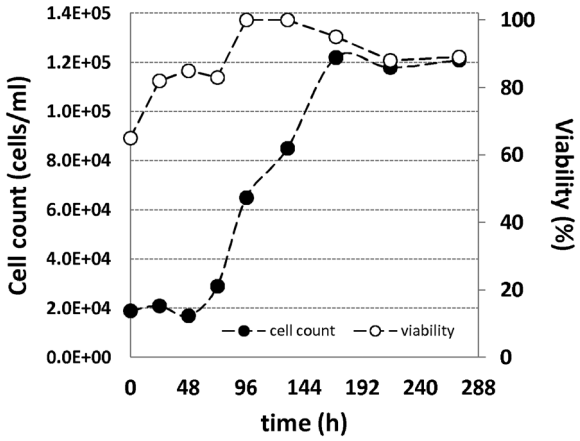

Figure 8. Culture of stem cells. Non-embryonic human hematopoietic stem cell growth in a 30 mL eccentric stirred tank system; cell growth profile (●) and cell viability (○) during a 12-day culture are presented.

on the exponential growth phase, was 31.46 h—a 19.18% increase from doubling time in stationary culture Petri dishes (standard culture protocol for this type of cell; Murugappan et al., 2010). Throughout the culture period, cell viability was maintained in the range of 80–100% (Fig. 8). In the exponential phase, cell viability values were sustained in the range of 95–100%, representing indirect evidence that the conditions of the flow field are acceptable to favor the survival and growth of extremely shear sensitive cells. In eccentric systems, although the highest velocity values are located near the impeller (see Figs. 3 and 4), a defined impeller discharge with very high and localized velocity values (and consequently shear values) is not observed (compare this with the concentric case in Fig. 4a). The lack of blades is partially responsible for lower stresses at impeller discharge. In addition, the use of an angled impeller motivates an oscillating motion in the impeller vicinity, helping to disperse the high shear effect to a wider area (see Fig. 4c).

Conclusions

In this study, we proposed a simple stirred tank system to be used as a mini-bioreactor for laboratory-scale experiments and low/medium-throughput screening applications. In this system, adequate mixing performance was achieved by the combined effect of three key elements: the eccentricity of the impeller shaft, the round bottom, and the inclination of the impeller disc. The eccentricity of the impeller shaft disrupted the flow symmetry, creating chaos, which is the main mixing mechanism in a laminar regime. The round bottom helped to eradicate the segregated regions that result when a flat-bottomed vessel is used. The third element, the use of a 45° angled-disc impeller, helped to create a more complex flow structure, enhancing axial flow. Mixing performance of this mini-bioreactor system was validated through experimental flow pattern visualization, using p-LIF and CFD simulations. The results revealed the complexity of the flow and mixing structure induced by the use of an off-centered and angled-disc impeller. The results from the culture of CHO cells and hematopoietic stem cells, suggest that this mini-bioreactor is suitable for small-scale mammalian cell culture experiments and reproduces meaningful process variables (namely specific growth rates, maximum cell concentrations) observable in larger-scale (1L) instrumented bioreactors.

The authors acknowledge the financial support provided by the Mexican government through CONACYT scholarships for D.B.A. and P.B.S.A. The authors are grateful for the financial support provided by Tecnológico de Monterrey at Monterrey through Cátedra de Investigación (CAT 122).

References

Ali S, Pérez-Pardo MA, Aucamp JP, Craig A, Bracewell DG, Baganz F. 2012. Characterization and feasibility of a miniaturized stirred tank bioreactor to perform *E. coli* high cell density fed-batch fermentations. Biotechnol Prog 28(1):66–75.

Alvarez MM. 2000. Using spatiotemporal asymmetry to enhance mixing in chaotic flows: From maps to stirred tanks. Ph D Thesis Chemical and Biochemical Engineering. Rutgers University: New Brunswick, NJ.

Alvarez MM, Arratia PE, Muzzio FJ. 2002a. Laminar mixing in eccentric stirred tank systems. Can J Chem Eng 80(4):546–557.

Alvarez MM, Zalc JM, Shinbrot T, Arratia PE, Muzzio FJ. 2002b. Mechanisms of mixing and creation of structure in laminar stirred tanks. AIChE J 48(10):2135–2148.

Alvarez-Hernández MM, Shinbrot T, Zalc JM, Muzzio FJ. 2002. Practical chaotic mixing. Chem Eng Sci 57(17):3749–3753.

Alvarez MM, Guzmán A, Elías M. 2005. Experimental visualization of mixing pathologies in laminar stirred tank bioreactors. Chem Eng Sci 60 (8–9 Spec. Iss.): 2449–2457.

Amanullah A, Buckland BC, Nienow AW. 2004. Mixing in the fermentation and cell culture industries. In: Paul EL, Atiemo-Obeng VA, Kresta SM, editors. Handbook of industrial mixing: Science and practice. Hoboken, NJ: Willey Interscience. p 1071–1170.

Amanullah A, Otero JM, Mikola M, Hsu A, Zhang J, Aunins J, Schreyer HB, Hope JA, Russo AP. 2010. Novel micro-bioreactor high troughput technology for cell culture process development: Reproducibility and scalability assessment of fed-batch CHO cultures. Biotechnol Bioeng 106(1):57–67.

Arratia P, Alvarez MM, Shinbrot T, Muzzio FJ. 2005. Three dimensional chaotic mixing. Phys Fluids 16(9):S8.

Ascanio G, Brito-Bazán M, Brito-De La Fuente E, Carreau PJ, Tanguy PA. 2002. Unconventional configuration studies to improve mixing times in stirred tanks. Can J Chem Eng 80(4):558–565.

Bareither R, Pollard D. 2011. A review of advanced small-scale parallel bioreactor technology for accelerated process development: Current state and future need. Biotechnol Prog 27(1):2–14.

Betts JI, Doig SD, Baganz F. 2006. Characterization and application of a miniature 10 mL stirred tank bioreactor showing scale-down equivalence with a conventional 7L reactor. Biotechnol Prog 22(3):681–688.

Bulnes-Abundis D. 2012. CFD as main tool for the characterization of mixing performance, shear stress distributions and adequacy for cell culture of stirred tanks agitated by eccentrically located inclined disks. Ph.D. Thesis. Tecnológico de Monterrey, Monterrey, NL, México.

Cabaret F, Fradette L, Tanguy PA. 2008. Effect of shaft eccentricity on the laminar mixing performance of a radial impeller. Can J Chem Eng 86(6):971–977.

Cascaval D, Galaction A-I, Oniscu C, Ungureanu F. 2004. Modeling of mixing in stirred bioreactors 4. Mixing time for aerated bacteria, yeast and fungus broths. Chem Ind 58(3):128–137.

Chisti Y. 2000. Animal-cell damage in sparged bioreactors. Trends Biotechnol 18(10):420–432.

Fernandes P, Carvalho F, Marques MPC. 2011. Miniaturization in biotechnology: Speeding up the development of bioprocesses. Recent Patents Biotechnol 5(3):160–173.

Galleti CH, Brunazzi E. 2008. On the main flow features and instabilities in an unbaffled vessel agitated with an eccentrically located impeller. Chem Eng Sci 63(18):4494–4505.

Gill NK, Appleton M, Baganz F, Lye GJ. 2008. Design and characterisation of a miniature stirred bioreactor system for parallel microbial fermentations. Biochem Eng J 39(1):164–176.

Godoy-Silva R, Chalmers JJ, Casnocha SA, Bass LA, Ma N. 2009. Physiological responses of CHO cells to repetitive hydrodynamic stress. Biotechnol Bioeng 103(6):1103–1117.

González-Leal IJ, Carrillo-Cocom LM, Ramírez-Medrano A, López-Pacheco F, Bulnes-Abundis D, Webb-Vargas Y, Alvarez MM. 2011. Use of a Plackett–Burman statistical design to determine the effect of selected amino acids on monoclonal antibody production in CHO cells. Biotechnol Prog 27(6):1709–1717.

Hobbs DM, Alvarez MM, Muzzio FJ. 1997. Mixing in globally chaotic flows: A self-similar process. Fractals 5(3):395–425.

Hu Y, Liu Z, Yang J, Cheng Y. 2010. Liquid mixing in eccentric stirred tank. Huagong Xuebao/CIESC J 61(10):2517–2522.

Karcz J, Cudak M, Szoplik J. 2005. Stirring of a liquid in a stirred tank with an eccentrically located impeller. Chem Eng Sci 60(8–9):2369–2380.

Keane JT, Ryan D, Gray PP. 2003. Effect of shear stress on expression of a recombinant protein by Chinese hamster ovary cells. Biotechnol Bioeng 81(2):211–220.

Kim JY, Kim Y-G, Lee G. 2012. CHO cells in biotechnology for production of recombinant proteins: Current state and further potential. Appl Microbiol Biotechnol 93(3):917–930.

Kovnov A, Tryggyason G, Khinast JG. 2007. Characterization of hydrodynamic shear forces and dissolved oxygen distribution in sparged bioreactors. Biotechnol Bioeng 97(2):317–331.

Kowalczyk M, Waldron K, Kresnowati P, Danquah MK. 2011. Process challenges relating to hematopoietic stem cell cultivation in bioreactors. J Ind Microbiol Biotechnol 38(7):761–767.

Lai Y, Yang M. 2010. Experiments on solid–liquid suspension in unbaffled stirred tank. Jiangsu Daxue Xuebao (Ziran Kexue Ban)/J Jiangsu University (Nat Sci Edition) 31(3):309–313.

Lamberto DJ, Álvarez MM, Muzzio FJ. 1999. Experimental and computational investigation of the laminar flow structure in a stirred tank. Chem Eng Sci 54:919.

Lamberto DJ, Alvarez MM, Muzzio FJ. 2001. Computational analysis of regular and chaotic mixing in a stirred tank reactor. Chem Eng Sci 56(16):4887–4899.

Marques MPC, Cabral JMS, Fernandes P. 2010. Bioprocess scale-up: Quest for the parameters to be used as criterion to move from microreactors to lab-scale. J Chem Technol Biotechnol 85(9):1184–1198.

Micheletti M, Lye GJ. 2006. Microscale bioprocess optimization. Curr Opin Biotechnol 17(6):611–618.

Montante G, Bakker A, Paglianti A, Magelli F. 2006. Effect of the shaft eccentricity on the hydrodynamics of unbaffled stirred tanks. Chem Eng Sci 61(9):2807–2814.

Mou DG. 2010. Short communication: Ambient gas exchange-enabled stirred culture bottle: A stirred tank reactor alternative to shake flasks for high gas–liquid mass transfer. Ind Biotechnol 6(2):100–103.

Morga-Ramírez M, Collados-Larrumbe MT, Johnson KE, Rivas-Arreola MJ, Carrillo-Cocom LM, Álvarez MM. 2010. Hydrodynamic conditions induce changes in secretion level and glycosylation patterns of Von Willebrand factor (vWF) in endothelial cells. J Biosci Bioeng 109(4):400–406.

Murugappan G, Carrillo-Cocom LM, Johnson KE, Bulnes-Abundis D, Zavala-Arcos J, Moreno-Cuevas JE, González-Garza MT, Alvarez MM. 2010. Human hematopoietic progenitor cells grow faster under rotational laminar flows. Biotechnol Prog 26(5):1465–1473.

Nienow AW. 2006. Reactor engineering in large scale animal cell culture. Cytotechnology 50(1–3):9–33.

Nienow AW. 2009. Scale-up considerations based on studies at the bench scale in stirred bioreactors. J Chem Eng Jpn 42(11):789–796.

Nikakhtari H, Hill GA. 2006. Closure effects on oxygen transfer and aerobic growth in shake flasks. Biotechnol Bioeng 95(1):15–21.

Rodrigues CAV, Fernandes TG, Diogo MM, da Silva CL, Cabral JMS. 2011. Stem cell cultivation in bioreactors. Biotechnol Adv 29(6):815–829.

Sánchez-Cervantes MI, Lacombe J, Muzzio FJ, Alvarez MM. 2006. Novel bioreactor design for the culture of suspended mammalian cells. Part 1: Mixing characterization. Chem Eng Sci 61(24):8075–8084.

Suresh S, Srivastava VC, Mishra IM. 2009. Critical analysis of engineering aspects of shaken flask bioreactors. Crit Rev Biotechnol 29(4):255–278.

Szoplik J, Karcz J. 2008. Mixing time of a non-Newtonian liquid in an unbaffled agitated vessel with an eccentric propeller. Chem Pap 62(1):70–77.

Takahashi K, Shigihara D, Takahata Y. 2011. Laminar mixing in eccentric stirred tank with different bottom. J Chem Eng Jpn 44(12):931–935.

Tanzeglock T, Soos M, Stephanopoulus G, Morbidelli M. 2009. Induction of mammalian cell death by simple shear and extensional flows. Biotechnol Bioeng 104(2):360–370.

Vallejos JR, Kostov Y, Ram A, French JA, Marten MR, Rao G. 2005. Optical analysis of liquid mixing in a bioreactor. Biotechnol Bioeng 93(5):906–911.

Want AJ, Nienow AW, Hewitt CJ, Coopman K. 2012. Large-scale expansion and exploitation of pluripotent stem cells for regenerative medicine purposes: Beyond the T flask. Regen Med 7(1):71–84.

Wen Y, Zang R, Zhang X, Yang ST. 2012. A 24-microwell plate with improved mixing and scalable performance for high throughput cell cultures. Process Biochem 47(4):612–618.

Woziwodzki S, Jedrzejczak Ł. 2010. Effect of eccentricity on laminar mixing in vessel stirred by double turbine impellers. Chem Eng Res Design 89(11):2268–2278.

Yang FL, Zhou SJ, Wng GC. 2011. Experimental study and detached eddy simulation of the macro-instability in an eccentric stirred tank. Appl Mech Mat 66–68:20–26.

Yang FL, Zhou SJ, Zhang CX, Chen LF. 2008. Investigation on solid–liquid suspension performance in an eccentrically stirred tank. Guochengg Gongcheng Xuebao 8(6):1064–1069.

Zalc JM, Szalai ES, Alvarez MM, Muzzio FJ. 2002. Using CFD to understand chaotic mixing in laminar stirred tanks. AIChE J 48(10):2124–2134.

Zhang H, Wang W, Quan C, Fan S. 2010. Engineering considerations for process development in mammalian cell cultivation. Curr Pharm Biotechnol 11(1):103–112.